SERIES ON PROGRESS IN HIGH TEMPERATURE SUPERCONDUCTIVITY

Published

Vol. 1 — Proceedings of the Adriatico Research Conference on High Temperature Superconductors (*eds. S. Lundqvist, E. Tosatti, M. Tosi and Yu Lu*)
Vol. 2 — Proceedings of the Beijing International Workshop on High Temperature Superconductivity (*eds. Z. Z. Gan, G. J. Cui, G. Z. Yang and Q. S. Yang*)
Vol. 3 — Proceedings of the Drexel International Conference on High Temperature Superconductivity (*eds. S. Bose and S. Tyagi*)
Vol. 4 — Proceedings of the 2nd Soviet-Italian Symposium on Weak Superconductivity (*eds. A. Barone and A. Larkin*)
Vol. 5 — High Temperature Superconductors — IX Winter Meeting on Low Temperature Physics (*eds. J. L. Heiras, R. A. Barrio, T. Akachi and J. Tagüeña*)
Vol. 7 — Chemical and Structural Aspects of High Temperature Superconductors (*ed. C. N. R. Rao*)
Vol. 8 — World Congress on Superconductivity (*eds. C. G. Burnham and R. Kane*)
Vol. 9 — First Latin-American Conference on High Temperature Superconductivity (*eds. R. Nicolsky, R. A. Barrio, R. Escudero and O. F. de Lima*)
Vol. 11 — High Temperature Superconductivity from Russia (*eds. A. I. Larkin and N. V. Zavaritsky*)
Vol. 12 — High Temperature Superconductivity and Other Related Topics — 1st Asia-Pacific Conference on Condensed Matter Physics (*eds. C. K. Chew et al.*)
Vol. 14 — Proceedings of the Adriatico Research Conference and Workshop on Towards the Theoretical Understanding of High Temperature Superconductors (*eds. S. Lundqvist, E. Tosatti, M. Tosi and Yu Lu*)
Vol. 15 — International Symposium on New Developments in Applied Superconductivity (*ed. Y. Murakami*)
Vol. 16 — Proceedings of the Srinagar Workshop on High Temperature Superconductivity (*eds. C. N. R. Rao et al.*)
Vol. 17 — Proceedings of High-T_c Superconductors: Magnetic Interactions (*eds. L. H. Bennett, Y. Flom and G. C. Vezzoli*)
Vol. 18 — Proceedings of the Tokai University International Workshop on the Science of Superconductivity and New Materials (*ed. S. Nakajima*)
Vol. 19 — Superconductivity and Applications — Taiwan International Symposium on Superconductivity (*eds. P. T. Wu et al.*)
Vol. 20 — High Temperature Superconductors — Xth Winter Meeting on Low Temperature Physics (*eds. T. Akachi et al.*)
Vol. 21 — Proceedings of the International Seminar on High Temperature Superconductivity (*eds. N. N. Bogolubov, V. L. Aksenov and N. M. Plakida*)
Vol. 22 — Proceedings of the 2nd Beijing International Workshop on High Temperature Superconductivity (*eds. Z. X. Zhao, G. J. Cui and R. S. Han*)
Vol. 23 — Proceedings of the Anniversary Adriatico Research Conference and Workshop on Strongly Correlated Electron Systems (*eds. G. Baskaran, A. E. Ruckenstein, E. Tosatti and Yu Lu*)
Vol. 24 — Proceedings of the European Conference on High-T_c Thin Films and Single Crystals (*eds. W. Gorzkowski et al.*)

Forthcoming

Vol. 13 — Applications of High Temperature Superconductors (*ed. C. Y. Huang*)
Vol. 26 — Proceedings of the XI Winter Meeting on Low Temperature Physics — Ceramic Superconductors (*eds. J. A. Cogordan et al.*)
Vol. 27 — Superconductivity — Proceedings of the XXIV Italian National School on Condensed Matter (*eds. S. Pace and M. Acquarone*)

Progress in High Temperature Superconductivity — Vol. 25

Proceedings of the ICTPS '90 International Conference on

TRANSPORT PROPERTIES OF SUPERCONDUCTORS

April 29—May 4 1990, Rio de Janeiro, Brazil

Editor

Roberto Nicolsky
Instituto de Fisica
Universidade Federal do Rio de Janeiro
Rio de Janeiro, Brazil

World Scientific
Singapore • New Jersey • London • Hong Kong

EXPERIMENTS ON ELECTRON- AND HOLE-DOPED HIGH T_c COPPER OXIDE SUPERCONDUCTORS

M. B. Maple, N. Y. Ayoub,[a] J. Beille,[b] T. Bjørnholm,[c] Y. Dalichaouch, E. A. Early, S. Ghamaty, B. W. Lee, J. T. Markert,[d] J. J. Neumeier,[e] G. Nieva, L. M. Paulius, I. K. Schuller, C. L. Seaman, and P. K. Tsai

Department of Physics and Institute for Pure and Applied Physical Sciences

University of California at San Diego, La Jolla, CA 92093 USA

ABSTRACT

Experiments on hole-doped $Y_{1-x}Pr_xBa_2Cu_3O_{7-\delta}$ and electron-doped $Ln_{2-x}M_xCuO_{4-y}$ (Ln = Pr, Nd, Sm, Eu, Gd; M = Ce, Th; $y \approx 0.02$) compounds are briefly reviewed. The hole-doped $Y_{1-x}Pr_xBa_2Cu_3O_{7-\delta}$ system exhibits a rich variety of phenomena including a metal-insulator transition at $x \approx 0.6$, high T_c superconductivity, anomalous behavior of the pressure dependence of T_c and the temperature dependence of the upper critical field, antiferromagnetic (AFM) ordering of Cu^{2+} and Pr ions, Kondo-like specific heat anomalies, and enormous electronic specific heat coefficients. The underlying cause of many of these phenomena appears to be associated with strong hybridization between the localized 4f states of Pr and the CuO_2 valence band states. Investigations on the electron-doped $Ln_{2-x}M_xCuO_{4-y}$ compounds suggest the existence of an electron-hole symmetry in the occurrence of the metal-insulator transition, Cu^{2+} AFM ordering, and superconductivity as a function of electron or hole donor concentration. Recent experiments on the electron-doped $Ln_{2-x}M_xCuO_{4-y}$ compounds reveal an electron-hole antisymmetry in the pressure dependence of T_c and the first example of the effect of AFM ordering on superconductivity in high T_c cuprates.

Introduction

The occurrence[1] of high T_c superconductivity in layered copper oxides has generated an enormous amount of interest in these remarkable materials. A broad and intense interdisciplinary research effort on both basic and applied aspects of high temperature superconductivity is currently underway on a worldwide scale. Although similar in many respects to conventional superconductors, the high-T_c materials display many unusual characteristics which both challenge theory and imbue these materials with the potential for wide-ranging technological applications. Noteworthy examples include extremely high superconducting critical temperatures T_c, small coherence lengths, enormous upper critical magnetic fields, and large anisotropy of various properties due to the layered structure.

(a) Permanent address: Department of Physics, Yarmouk University, Irbid, Jordan.

(b) Permanent address: Laboratorie Louis Néel, CNRS, 25 Avenue des Martyrs, 166X, 38042 Grenoble CEDEX, France.

(c) Permanent address: Center of Interdisciplenary Studies of Molecular Interactions, University of Copenhagen, Bledanusuej 21, DK 2100 0, Copenhagen, Denmark.

(d) Present address: Department of Physics, University of Texas, Austin, TX 78712 USA.

(e) Present address: Sektion-Physik, Universität München, Schellingstraße 4/V. 8000 München, 40, FRG.

One of the outstanding problems in this field of research is the role of charge carrier concentration in controlling the superconducting and magnetic properties and their mutual interaction. In all high T_c copper oxide systems discovered so far, superconductivity lies in a relatively narrow range of carrier concentration, between insulating antiferromagnetic behavior and metallic, Fermi liquid like behavior. The role of the carriers is particularly interesting in the $Y_{1-x}Pr_xBa_2Cu_3O_{7-\delta}$ and electron-doped superconductors. For the $Y_{1-x}Pr_xBa_2Cu_3O_{7-\delta}$ system, Pr appears to contribute electrons to the CuO_2 planes, which reduces the concentration of mobile holes, driving the system nonmetallic and onsuperconducting for $x \geq 0.6$. The electron-doped system is the first among the copper xide superconductors in which the charge carriers appear to be electrons, rather than noles, which could place serious constraints on viable theories for high temperature superconductivity.

Furthermore, many of the high T_c materials are new examples of magnetic superconductors in which there is coexistence of rare-earth magnetic order and superconductivity. For both $Y_{1-x}Pr_xBa_2Cu_3O_{7-\delta}$ and the electron-doped materials, there is compelling evidence for significant interactions between the rare-earth ions and the superconducting charge carriers which can have dramatic effects on the superconducting properties.

The Hole-doped System $Y_{1-x}Pr_xBa_2Cu_3O_{7-\delta}$

Among the rare earth R elements that form the series of $RBa_2Cu_3O_{7-\delta}$ ($\delta \approx 0.1$) compounds with the orthorhombic Pmmm crystal structure (R = Y or a lanthanide except Ce, Pm, and Tb), only Pr yields a nonmetallic and nonsuperconducting compound; the compounds of all of the other R elements are metallic and superconducting with superconducting critical temperatures T_c that range[2] from ~92 K to ~95 K. The origin of the nonmetallic character of $PrBa_2Cu_3O_{7-\delta}$ is of considerable interest and could provide useful information concerning the electronic structure of the metallic $RBa_2Cu_3O_{7-\delta}$ compounds and, in turn, the occurrence of high T_c superconductivity in these remarkable materials.

During the past several years, we have been involved in an extensive investigation[3] of Pr in the pseudoquaternary system $Y_{1-x}Pr_xBa_2Cu_3O_{7-\delta}$, in which a rich variety of phenomena are found. The superconducting critical temperature T_c decreases with x and vanishes at $x \approx 0.6$, near the composition where a metal-insulator transition occurs.[4,5,6] Two mechanisms for the suppression of T_c with x in the $Y_{1-x}Pr_xBa_2Cu_3O_{7-\delta}$ system that have been considered are (1) the filling of mobile holes in the CuO_2 planes by electrons contributed by Pr ions with a valence greater than the valence (+3) of the Y ions,[4,5,6] and (2) the spin-dependent exchange scattering of mobile holes in the CuO_2 planes by the Pr ions[7,8,9]. One or both of these mechanisms could be operative in this system.[10] Anomalous behavior has been observed in the pressure dependence of T_c (Ref. 7) and the temperature dependence of the upper critical field H_{c2} (Ref. 11) in the $Y_{1-x}Pr_xBa_2Cu_3O_{7-\delta}$ system. The low temperature specific heat due to the Pr ions can be described by the sum of a Pr nuclear Schottky anomaly, a large linearly temperature dependent term, and a magnetic contribution.[12] In the metallic state ($0 \leq x \lesssim 0.6$), the magnetic contribution takes the form of a Kondo anomaly, whereas in the insulating state ($0.6 \lesssim x \leq 1.0$), the magnetic contribution is associated with antiferromagnetic (AFM) ordering of the Pr ions which takes place in a background of Cu^{2+} AFM ordering.

The underlying cause of the above effects appears to be moderately strong hybridization between the localized 4f electron states of Pr and CuO_2 valence band states.[3,7,13] The Pr 4f-CuO_2 valence band hybridization could provide a means for (1) transferring electrons from Pr ions to the CuO_2 planes, and (2) generating a large negative

(antiferromagnetic) exchange interaction between the spins of the mobile holes in the CuO_2 planes and the Pr magnetic moments. An important issue which remains to be resolved concerns the valence of the Pr ions; for example, crystallographic,[14] electrical transport,[15,16] magnetic,[6,11] and thermal[12] measurements suggest a valence close to +4, whereas spectroscopic data[13,17] generally yield a valence close to +3.

Hole Filling and Pair Breaking in the $Y_{1-x}Pr_xBa_2Cu_3O_{7-\delta}$ System

The T_c vs x curve for the $Y_{1-x}Pr_xBa_2Cu_3O_{7-\delta}$ system, based upon recent measurements,[11,12] is shown in Fig. 1. The curve has a very characteristic shape which consists of an initial flat portion, followed by a linear decrease in the range $0.1 \lesssim x \lesssim 0.55$, and a more rapid drop to zero at $x \approx 0.6$ which is probably related to the occurrence of the metal-insulator transition indicated by the dashed line in Fig. 1. Also shown in Fig. 1 are the temperatures of the maxima in the specific heat in the metallic region, discussed below, and the Néel temperatures deduced from specific heat data for antiferromagnetic (AFM) ordering of the Pr ions in the insulating region. The AFM ordering of the Pr ions takes place in a background of Cu^{2+} AFM ordering that occurs at higher temperatures,[18,19] as depicted in Fig.1.

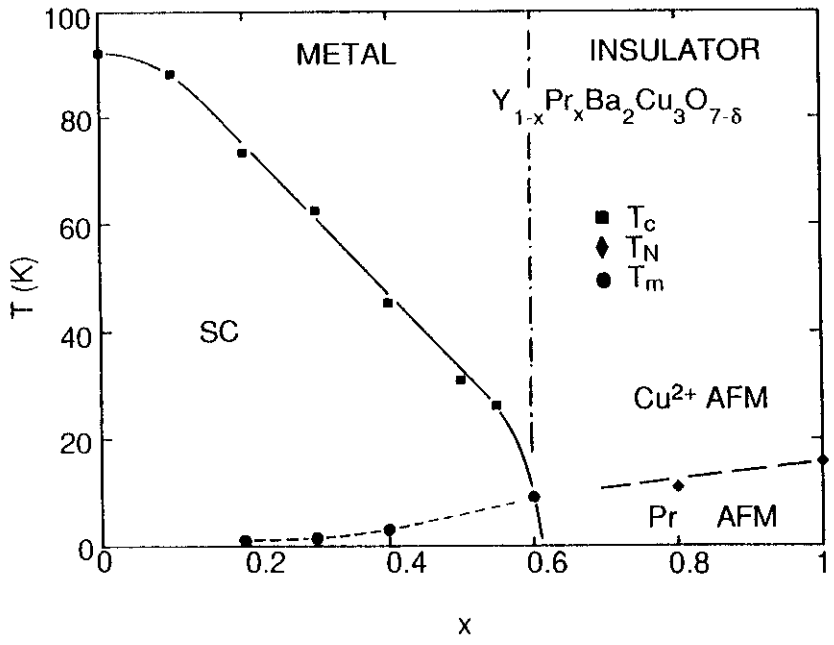

Fig.1. Temperature–Pr concentration (T-x) phase diagram for the $Y_{1-x}Pr_xBa_2Cu_3O_{7-\delta}$ system. From Ref. 12.

Recently, we probed the superconductivity in the $Y_{1-x}Pr_xBa_2Cu_3O_{7-\delta}$ system[10] by substituting divalent Ca ions for trivalent Y ions to form the system $(Y_{1-x-y}Ca_y)Pr_xBa_2Cu_3O_{7-\delta}$. Curves of T_c vs Ca concentration y for fixed values of the Pr concentration x of 0, 0.1, 0.15, and 0.2 were determined experimentally and are shown in Fig. 2. The T_c vs y curves exhibit maxima for x = 0.15 and 0.2 which are observed to shift to lower values of T_c and higher values of y with increasing Pr concentration x.

We found that the overall behavior of the T_c vs y curves for fixed values of x could be described by the expression

$$T_c(x,y) = T_{co} - A(\alpha-\beta x+y)^{\gamma} - Bx \qquad (1)$$

In Eq. 1, T_{co} is the maximum attainable value of T_c, $-A(\alpha-\beta x+y)^{\gamma}$ is an empirical term that was interpreted in terms of hole generation by Ca (y) ions and hole filling by Pr (x) ions, $-\alpha$ is optimal hole concentration, β is the deviation of the effective valence of Pr, v(Pr), from +3 [i.e., β = v(Pr)-3], and -Bx describes the overall depression of T_c with x which was attributed to pair breaking interactions. The best overall fit of Eq. 1 to the $T_c(x,y)$ data

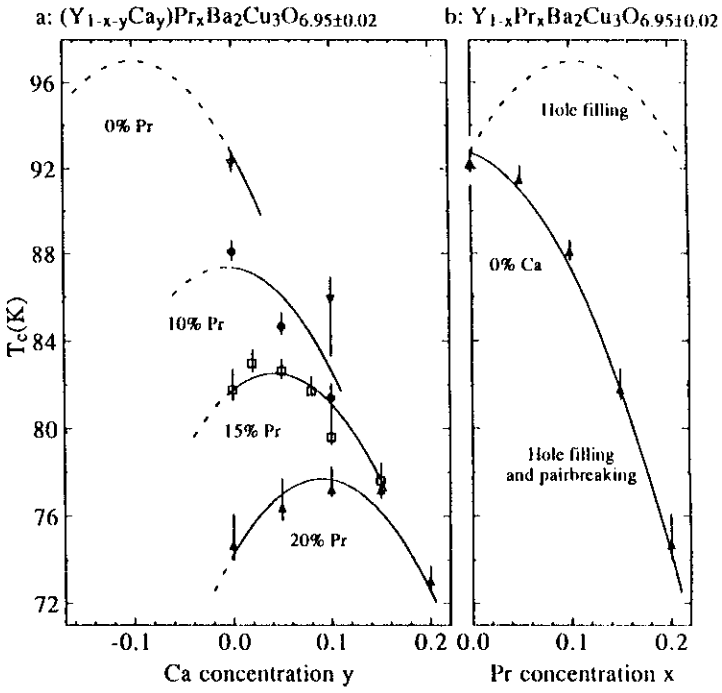

Fig. 2. (a) T_c vs Ca concentration y for four Pr concentrations x. Curves formed by solid and dashed lines represent Eq. 1 in the text. The negative Ca concentrations are hypothetical and would correspond to tetravalent substitutions. (b) T_c vs Pr concentration x. The dashed line represents the function $T_c(x,y = 0)$ + (96.5 K)x which describes pure hole filling and the solid line represents the function $T_c(x,y = 0)$ which includes hole filling and pair breaking. From Ref. 10.

gives the following values for these parameters: T_{CO} = 97 K, A = 425 K, α = 0.10, β = 0.95 ± 0.20, γ = 2, and B = 96.5 K. The value obtained for β yields v(Pr) = 3+β = 3.95 ± 0.20, suggesting that the Pr ions are nearly tetravalent. This result is consistent with magnetic susceptibility measurements[6,11] on the $Y_{1-x}Pr_xBa_2Cu_3O_{7-\delta}$ system throughout the range $0 \leq x \leq 1$, the results of which can be described by the sum of a constant Pauli-like term and a Curie-Weiss law with an effective moment[11] of ~2.5 μ_B, close to the 2.54 μ_B Hund's rules value for a single f-electron (tetravalent Pr). The magnitude of the exchange interaction parameter $\mathcal{J}$ can be estimated from the value of B by using a pair breaking theory such as that of Abrikosov and Gor'kov (AG)[20] in which the exchange scattering rate is calculated to second order in $\mathcal{J}$, or one that takes into account the Kondo effect (exchange scattering to higher order than $\mathcal{J}^2$). The AG result is adequate for an order of magnitude estimate of $|\mathcal{J}|$ and for low values of x is given by

$$T_c(x) \approx T_{CO} - |(\pi^2/4k_B)N(E_F)\mathcal{J}^2(g_J - 1)^2J(J+1)|x = T_{CO} - Bx \qquad (2)$$

where $N(E_F)$ is the density of states at the Fermi level and g_J and J are, respectively, the Landé g-factor and total angular momentum of the Hund's rules ground state of the Pr

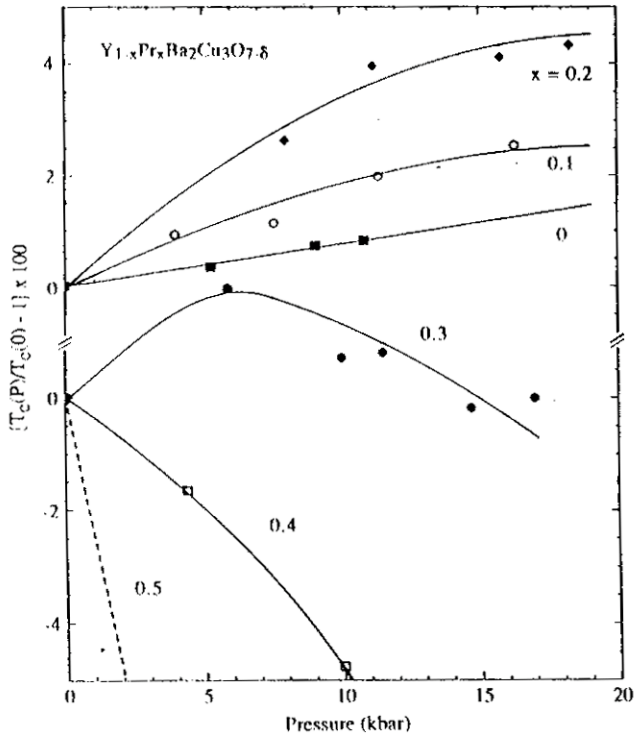

Fig. 3. T_c vs pressure P for $Y_{1-x}Pr_xBa_2Cu_3O_{7-\delta}$ compounds with x = 0, 0.1, 0.2, 0.3, 0.4 and 0.5. From Ref. 7.

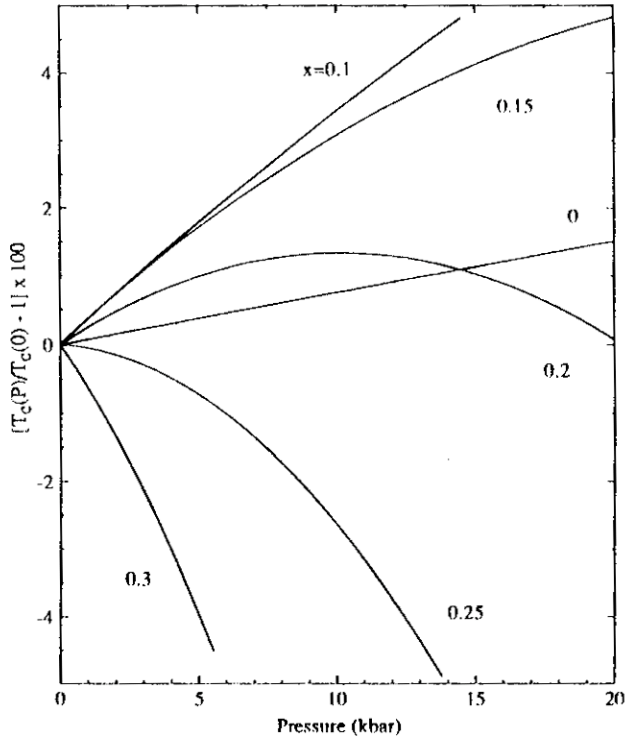

Fig. 4. Calculated T_c vs pressure P curves for $Y_{1-x}Pr_xBa_2Cu_3O_{7-\delta}$ with x = 0, 0.10, 0.15, 0.20, 0.25, 0.30. From Ref. 21.

ions. Using the value $N(E_F) \approx 11.5$ states/eV, $g_J = 0.86$, and J = 5/2 for Pr^{4+}, a value of ~41 meV is obtained for |J|.

An extension of Eq. 1 to incorporate the effect of applied pressure P can also account qualitatively for the striking variations of T_c with P that have been observed in the $Y_{1-x}Pr_xBa_2Cu_3O_{7-\delta}$ system.[21] Shown in Fig. 3 are T_c vs P data for $Y_{1-x}Pr_xBa_2Cu_3O_{7-\delta}$ specimens with Pr concentrations x of 0, 0.1, 0.2, 0.3, 0.4, and 0.5.[7] The data reveal a striking crossover from positive to negative pressure dependences of T_c as the Pr concentration is increased. These trends in the $T_c(x,P)$ data can be obtained from Eq. 1 by assuming that the parameters A, α, and γ are, to a first approximation, independent of P, T_{co} has the same pressure dependence as pure $YBa_2Cu_3O_{7-\delta}$, and β and B can be expanded in a power series to first order in P; i.e.,

$$T_{co}(P) \approx T_{co}(0) + (0.07\ K/kbar)P \tag{3}$$

$$\beta(P) \approx \beta(0) + \beta'(0)P \tag{4}$$

$$B(P) \approx B(0) + B'(0)P \tag{5}$$

The best overall fit of the resultant expression for $[dT_c(x,P)/dP]_{P=0}$ to the experimental data yields the values $\beta'(0) = 0.024$ kbar^{-1} and $B'(0) = -2.45$ K kbar^{-1}. The increase of β with P indicates that ν(Pr) increases with P, which is intuitively reasonable. A decrease (increase) of |J| with P can be inferred from the decrease of B'(0) with P, depending upon whether the complications associated with the Kondo effect are excluded (included). The Kondo effect is expected (and apparently observed in the specific heat of the $Y_{1-x}Pr_xBa_2Cu_3O_{7-\delta}$ system, as discussed below) in metals containing R ions that carry magnetic moments when there is strong hybridization between the localized 4f states of the R ion and conduction electron states which generates a large, negative (antiferromagnetic) exchange interaction.[20] However, inclusion of the Kondo effect in the analysis of the $T_c(x,P)$ data is complicated and beyond the scope of the present work.

The calculated $T_c(x,P)$ curves for x values of 0, 0.10, 0.15, 0.20, 0.25, and 0.30 are shown in Fig. 4. The calculated $T_c(x,P)$ curves give a good qualitative description of the overall trends in the experimental $T_c(x,P)$ data shown in Fig. 3, although the x values of the calculated and experimental curves do not correspond exactly with one another.

If the Pr valence is actually close to +3, as indicated by the spectroscopic data, the analysis of the $T_c(x,y,P=0)$ and $T_c(x,y=0,P)$ data for the $Y_{1-x}Pr_xCa_yBa_2Cu_3O_{7-\delta}$ system discussed above would still be tenable, except that the parameters α and β in Eq. 1 would have different meanings. The parameter α would now be interpreted as the optimal concentration of mobile holes in the CuO_2 planes, while β would be a coefficient representing the fraction of a hole in the CuO_2 planes localized per Pr ion. The mechanism by means of which nearly one hole in the CuO_2 planes per substituted Pr ion becomes localized is not readily apparent, but would presumably be associated with the Pr 4f-CuO_2 valence band hybridization. According to recent EELS measurements[22] of the O 1s absorption edge in the $Y_{1-x}Pr_xBa_2Cu_3O_{7-\delta}$ system, the number of holes on the O sites is independent of x, suggesting that the Pr ions localize, rather than fill, holes in the CuO_2 planes.

Kondo Anomalies in the Low Temperature Specific Heat

In a metallic environment, the negative exchange interaction should give rise to the Kondo effect in which a many body singlet state involving the mobile holes and the Pr 4f electrons gradually forms as the temperature is lowered through the Kondo temperature T_K. Indeed, Kondo-type anomalies have been observed[12] in the specific heat of $Y_{1-x}Pr_xBa_2Cu_3O_{7-\delta}$ compounds at low temperatures for Pr concentrations in the metallic region $0 \le x \le 0.6$. In the insulating region, specific heat anomalies associated with AFM ordering of the Pr ions in a background of Cu^{2+} AFM ordering are observed. The Pr contribution to the low temperature specific heat, ΔC, of $Y_{1-x}Pr_xBa_2Cu_3O_{7-\delta}$ compounds with x = 0.2, 0.3, 0.4, and 0.6 between 0.5 K and 10 K, obtained by subtracting the specific heat of the $YBa_2Cu_3O_{7-\delta}$ background from the total specific heat, is shown in Fig. 5.[12]

The $\Delta C(T)$ data in Fig. 5 can be described by the sum of three contributions, a Pr nuclear Schottky anomaly $C_N(T)$, a linear term $C_L(T)$, and a Kondo anomaly $C_K(T)$; i.e.,

$$\Delta C(T) = C_N(T) + C_L(T) + C_K(T) \tag{6}$$

The Pr nuclear Schottky anomaly is assumed to take the form

$$C_N(T) = AT^{-2} \tag{7}$$

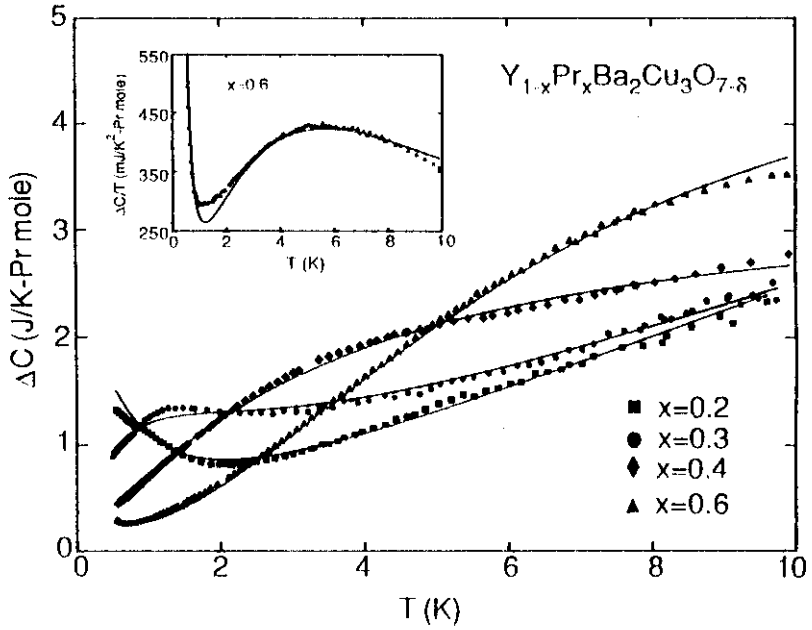

Fig. 5. Pr contribution to the specific heat ΔC vs temperature T for $Y_{1-x}Pr_xBa_2Cu_3O_{7-\delta}$ with $x \leq 0.6$. The inset shows ΔC/T vs T in a more extended temperature range for the sample with x = 0.6. The solid lines represent fits which include nuclear Schottky, linear and Kondo contributions. From Ref. 12.

while the linear term is given by

$$C_L(T) = \gamma T \tag{8}$$

For the Kondo specific heat anomaly, we use an expression provided by a static scaling model[23]

$$C_K(T) = (D/T)^2[1 + (T_K/T)]^{-\alpha} \tag{9}$$

The parameter D can be obtained from the entropy $R\ell n(2S+1)$ and is given by

$$D = (1 - \alpha)(2 - \alpha)T_K^2 R\ell n(2S + 1) \tag{10}$$

where R is the universal gas constant and the spin S is taken to be 1/2, which is appropriate for Pr ions which are tetravalent and have a doublet ground state in the presence of the crystalline electric field.

Least squares fits of Eqs. 6 - 10 to the ΔC(T) data for the $Y_{1-x}Pr_xBa_2Cu_3O_{7-\delta}$ specimens with x = 0.2, 0.3, 0.4, and 0.6 are shown in Fig. 5 and are seen to give a good description of the ΔC(T) data. For the Kondo specific heat anomaly, the best fits were obtained with $\alpha = 3$ and yielded values for T_K of 0.5, 2.1, and 15.4 K for x = 0.2, 0.3,

and 0.4, respectively. The x = 0.6 sample was fitted with $\alpha = 5$ and $T_K = 8.5$ K. Eqs. 9 and 10 were derived using the classical scaling hypothesis for second order phase transitions, extended to negative values of the critical temperature T_c (in our case, $T_c = -T_K$). With this description, the "critical exponent" α is restricted to values $\alpha > 2$. The large value of α needed to fit the x = 0.6 $\Delta C(T)$ data may be related to interactions between the Pr magnetic moments which become stronger in the insulating phase. The apparent increase of T_K with x is noteworthy and may be due to an increase of the magnitude of the Pr 4f-CuO_2 valence band hybridization which results in an increase in |J| and, in turn, $T_K \approx T_F \exp(-1/N(E_F)|J|)$, as well as interactions between the Pr magnetic moments. The coefficient γ of the linear term is of the order of 240 mJ/mole Pr-K^2 for x = 0.2 and 0.3 and 100 mJ/molePr-K^2 for x = 0.4 and 0.6, reminiscent of heavy fermion behavior. The existence of such a large linear "electronic-like" contribution is surprising and not well understood.[8,12] The Pr contribution to the specific heat of the insulating samples with x = 0.8 and 1.0, which lie in the insulating regime, can be described by Eq. 6, but with $C_K(T)$ replaced by an AFM magnon term of the form $C_M(T) = MT^3$ associated with the AFM order exhibited by the Pr ions.

The Electron-doped System $Ln_{2-x}M_xCuO_{4-y}$ (Ln = Pr, Nd, Sm, Eu, Gd; M = Ce, Th; y ≈ 0.02)

Prior to 1989, the prevailing view was that the charge carriers responsible for superconductivity in all high temperature superconducting oxides with $T_c > 30$ K were mobile holes confined to the conducting CuO_2 planes, the basic building blocks of these materials.[24] However, this view has been challenged by the discovery of new superconducting materials[25-27] in which the charge carriers involved in the superconductivity appear to be electrons which reside within the conducting CuO_2 planes.[28] These findings could have important implications regarding viable theories of high temperature superconductivity and strategies for finding new superconducting materials.

The new electron-doped superconducting materials are obtained by doping the parent compound Ln_2CuO_{4-y} by a variety of means, which are categorized in Table 1 along with the highest onset superconducting critical temperatures T_c for each specific compound. These dopings all appear to donate electrons to the CuO_2 planes from sites either within or outside the planes. The first, and largest, group of these materials has the chemical formula $Ln_{2-x}M_xCuO_{4-y}$, where M^{4+} ions are substituted for Ln^{3+} ions, thereby donating electrons from outside the CuO_2 planes, which results in T_c's as high as ~25 K for x ≈ 0.15 and y ≈ 0.02. Superconductivity has been discovered for M = Ce and Ln = Pr,[25] Nd,[25] Sm,[25] and Eu,[29] and for M = Th and Ln = Pr,[29] Nd,[26] and Sm.[30] A set with but one known superconducting member, $Nd_2CuO_{4-x-y}F_x$, displays superconductivity[27] with $T_c \approx 25$ K. Here, F^{1-} ions are substituted for O^{2-} ions, either within or outside the CuO_2 planes. The final, very recent, category contains compounds with the formula $Nd_{2-x}Ce_xCu_{1-z}M'_zO_{4-y}$, where M' = Ga^{3+} (Ref. 31) or In^{3+} (Ref. 32) ions substitute for Cu^{2+} ions within the CuO_2 planes. For x+z = 0.15, superconductivity has been observed with $T_c \approx 25$ K.

T-x phase diagrams : Electron/hole symmetry

The $Ln_{2-x}M_xCuO_{4-y}$ electron-doped superconductors have the same chemical formula as the $La_{2-x}M_xCuO_{4-y}$ hole-doped compounds, the class of materials in which evidence for high T_c superconductivity was first reported by Bednorz and Müller.[1] Whereas the

"T-phase" structure which is similar except that the copper ions are surrounded by an octahedral arrangement of oxygen ions.

There are also striking similarities between these two systems. Both parent compounds are antiferromagnetic insulators in which the Cu^{2+} magnetic moments order antiferromagnetically below ~300 K (Refs. 33 - 36) and ~280 K (Refs. 2, 33) for the T-phase and T'-phase compounds, respectively. As more charge carriers in the CuO_2 planes are generated by increasing the dopant concentration x, each material evolves from an insulator into a metal, the Cu^{2+} antiferromagnetism is suppressed, and each compound becomes superconducting with a maximum T_c and maximum flux expulsion (Meissner effect) at $x \approx 0.15$.

These results suggest there is an electron-hole symmetry in the occurrence of the insulator-metal transition, magnetism, and superconductivity in copper oxides as a function of the concentration of charge carriers in the CuO_2 planes. This is illustrated in Fig. 6 where the temperature—dopant concentration (T-x) phase diagrams delineating the regions of superconductivity and antiferromagnetic ordering of the Cu^{2+} ions are displayed for the hole-doped $La_{2-x}Sr_xCuO_{4-y}$ and electron-doped $Nd_{2-x}Ce_xCuO_{4-y}$ systems. The superconducting phase boundaries for the $La_{2-x}Sr_xCuO_{4-y}$ and $Nd_{2-x}Ce_xCuO_{4-y}$ systems are

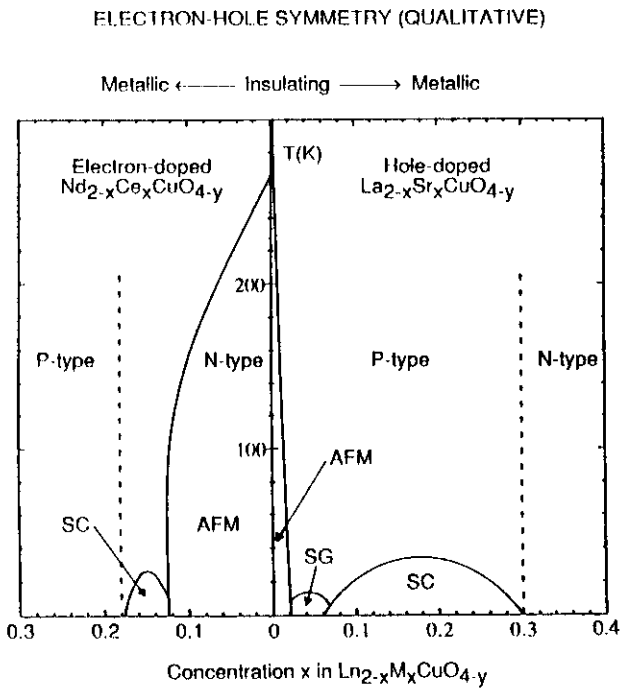

Fig. 6. Temperature–dopant concentration (T-x) phase diagram delineating the regions of superconductivity and antiferromagnetic ordering of the Cu^{2+} ions for the hole-doped $La_{2-x}Sr_xCuO_{4-y}$ and electron-doped $Nd_{2-x}Ce_xCuO_{4-y}$ systems. The symbols AFM, SG, and SC denote antiferromagnetic, spin-glass, and superconducting phases, respectively.

"T-phase" structure which is similar except that the copper ions are surrounded by an octahedral arrangement of oxygen ions.

There are also striking similarities between these two systems. Both parent compounds are antiferromagnetic insulators in which the Cu^{2+} magnetic moments order antiferromagnetically below ~300 K (Refs. 33 - 36) and ~280 K (Refs. 2, 33) for the T-phase and T'-phase compounds, respectively. As more charge carriers in the CuO_2 planes are generated by increasing the dopant concentration x, each material evolves from an insulator into a metal, the Cu^{2+} antiferromagnetism is suppressed, and each compound becomes superconducting with a maximum T_c and maximum flux expulsion (Meissner effect) at $x \approx 0.15$.

These results suggest there is an electron-hole symmetry in the occurrence of the insulator-metal transition, magnetism, and superconductivity in copper oxides as a function of the concentration of charge carriers in the CuO_2 planes. This is illustrated in Fig. 6 where the temperature—dopant concentration (T-x) phase diagrams delineating the regions of superconductivity and antiferromagnetic ordering of the Cu^{2+} ions are displayed for the hole-doped $La_{2-x}Sr_xCuO_{4-y}$ and electron-doped $Nd_{2-x}Ce_xCuO_{4-y}$ systems. The superconducting phase boundaries for the $La_{2-x}Sr_xCuO_{4-y}$ and $Nd_{2-x}Ce_xCuO_{4-y}$ systems are

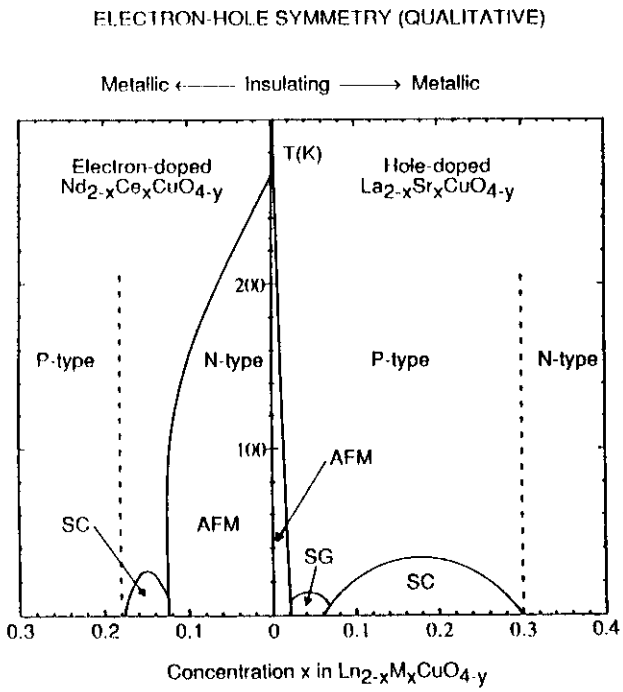

Fig. 6. Temperature–dopant concentration (T-x) phase diagram delineating the regions of superconductivity and antiferromagnetic ordering of the Cu^{2+} ions for the hole-doped $La_{2-x}Sr_xCuO_{4-y}$ and electron-doped $Nd_{2-x}Ce_xCuO_{4-y}$ systems. The symbols AFM, SG, and SC denote antiferromagnetic, spin-glass, and superconducting phases, respectively.

from Torrance et al.[37] and Ayoub et al.,[38] respectively, while the magnetic phase boundaries are based on muon spin relaxation studies by Uemura and coworkers.[33,34] The regions in the figure denoted "N-type" and "P-type" refer to electron and hole carriers, respectively, as inferred from the sign of the Hall coefficient measured on ceramic samples between 80 K and 300 K.[39,40] The symmetry in the crossover from N- to P-type and P- to N-type as a function of dopant concentration for the electron-and hole-doped systems is particularly striking. It is interesting that recent Hall effect measurements on $Nd_{2-x}Ce_xCuO_{4-y}$ single crystals yield a change from negative to positive Hall coefficients at low temperatures in some specimens,[41] indicating that the interpretation of Hall effect measurements in these materials is probably not straight forward.

The concentration range within which superconductivity occurs in the electron-doped $Nd_{2-x}Ce_xCuO_{4-y}$ system[38] is much narrower than that of the hole-doped $La_{2-x}Sr_xCuO_{4-y}$ system[37]. This may be related to the persistence of Cu-Cu antiferromagnetic (AFM) correlations to much higher dopant concentrations in the electron-doped materials[34-36] compared to the hole-doped $La_{2-x}Sr_xCuO_4$ compounds.[42] In a localized picture, such behavior can be qualitatively understood as follows. A doped hole, with appreciable oxygen 2*p* character and an associated spin may result in "spin frustration" for its two neighboring Cu^{2+} ions, leading to a rapid suppression of Cu-Cu AFM spin correlations with increasing doping; electron-doping, on the other hand, may predominantly result in the generation of Cu^{1+} and thus simply provide non-magnetic dilution, with an expectedly weaker effect[43] on the copper Néel temperature.

There is still considerable confusion in the literature regarding whether the charge carriers involved in the superconductivity of the electron-doped $Ln_{2-x}M_xCuO_{4-y}$ compounds actually are electrons. For example, x-ray photoemission spectroscopy (XPS)[44,45] and x-ray absorption spectroscopy (XAS)[46] studies indicate increasing Cu^{1+} with doping, while other XPS[47] and XAS[48] studies find no evidence for Cu^{1+}. XPS[47,49] and electron energy-loss spectroscopy[50] experiments suggest the presence of oxygen 2*p* holes. Furthermore, a band structure calculation[51] shows only a simple structure near the Fermi level, which is crossed by a single free-electron-like Cu-O antibonding $dp\sigma$ band. Finally, a recent resonant photoemission spectroscopy study[52] reveals that the Fermi level lies in states that fill in the x = 0 insulator gap.

A related question is the possible intermediate-valent nature of the Ce dopant ions. XAS,[46] x-ray diffraction,[53] and combined x-ray diffraction and XPS [54] investigations conclude a Ce valence intermediate between +3 and +4. However, two core-level XPS studies[49,55] and a composition-dependent study[38] of $Ln_{2-x}M_xCuO_{4-y}$ for M = Ce and Th indicate that Ce displays simple tetravalent behavior.

Gd as a Probe of Copper Antiferromagnetic Order

Although $Gd_{2-x}M_xCuO_{4-y}$ forms the T'-phase crystal structure, superconductivity has not been found in this system. This could be due to the smaller size or larger magnetic moment of Gd^{3+} compared to the lighter trivalent lanthanide ions. Another possibility is that the antiferromagnetic (AFM) correlations between the copper ions which suppress superconductivity are larger in this system. This might occur if a sufficient amount of oxygen could not be removed in the final reduction anneal. A slight oxygen deficiency is necessary to induce superconductivity in the electron-doped compounds, which might also destroy the Cu AFM order. Indeed, the final reduction anneal for $Gd_{2-x}M_xCuO_{4-y}$ is limited to less than ~825 °C, lower than for the other Ln's; higher reduction temperatures introduce impurity phases. For such a reduced $Gd_{1.85}Ce_{0.15}CuO_{4-y}$ sample, Cu AFM order occurs[35] below ~150 K.

Although not superconducting, the $Gd_{2-x}M_xCuO_{4-y}$ system exhibits a rich variety of magnetic phenomena[35,36,56] including Cu AFM order in the basal plane, Gd AFM order, and weak ferromagnetic (WFM) behavior which is induced by application of a small magnetic field in the basal plane direction below the Néel temperature T_N of the Cu moments. The onset of WFM at T_N results in a jump in the magnetization M at T_N. This can be understood in terms of an antisymmetric exchange interaction, as discussed by Dzyaloshinski[57] and Moriya,[58] in which a field-induced canting of the ordered Cu moments in the basal plane results in an increase in the effective magnetic field at the Gd site, thereby producing the jump in M. This WFM behavior is not seen in the Ln = Pr, Nd, or Sm $Ln_{2-x}M_xCuO_{4-y}$ systems;[59] however, it is seen in mixed $(Ln,Gd)_{2-x}Ce_xCuO_{4-y}$ systems with sufficient Gd concentration.

We have recently attempted to utilize the jump in M associated with the WFM behavior to determine the copper T_N in various electron-doped systems by doping with a small amount of Gd, which serves as a probe of the magnetic environment, and measuring the temperature at which there is a jump in the magnetization. Since only a small amount of Gd is necessary to produce a measurable jump in the $(Eu,Gd)_{2-x}Ce_xCuO_{4-y}$ system, we performed a series of experiments on $(Eu_{1.8-x}Gd_{0.2})Ce_xCuO_{4-y}$ to obtain T_N vs Ce concentration x. We found that T_N drops with increasing x, similarly to $Nd_{2-x}Ce_xCuO_{4-y}$ as determined from zero-field μSR measurements,[34] but our samples showed a saturation of T_N with x at ~150 K near x = 0.15. We were unable to induce superconductivity in any of these samples; it is difficult to make $Eu_{1.85}Ce_{0.15}CuO_{4-y}$ superconducting. It would be interesting to see if T_N vanishes when superconductivity appears.

Since $Nd_{2-x}Ce_xCuO_{4-y}$ has superior superconducting properties among the electron-doped compounds, we performed similar experiments on the $(Nd,Gd)_{2-x}Ce_xCuO_{4-y}$ system. However, we could not measure T_N vs Ce concentration because the WFM behavior disappears completely, even with optimum Ce concentration of 0.15, for Gd concentrations less than ~65%. We therefore decided to study superconductivity, Cu AFM order, and WFM as a function of Gd concentration. The results of this study are summarized as a temperature – Gd concentration (T-x) phase diagram shown in Fig. 7.

In Fig. 7, the triangles represent resistively determined T_c's of $(Nd_{1.85-x}Gd_x)Ce_{0.15}CuO_{4-y}$ compounds. Superconductivity is completely supressed between 50% and 65% Gd substituted for Nd. The closed circles represent temperatures at which anomalies are observed in the magnetization for various Gd concentrations x for $Nd_{2-x}Gd_xCuO_{4-y}$, whereas the squares depict anomalies for Ce-doped $(Nd_{1.85-x}Gd_x)Ce_{0.15}CuO_{4-y}$. The magnitudes of these anomalies decrease as x decreases from x = 2. Open symbols indicate Gd concentrations in which the anomalies are no longer discernible. The circles at 280 K represent the copper Néel temperatures of the Ce-undoped system. This Cu AFM order seems to be universal among the parent compounds; its existence in Nd_2CuO_{4-y} has been verified by μSR measurements[34] as represented by the open circle at 280 K for x = 0. We assume it also exists for intermediate Gd doping as indicated by the dotted line at T = 280 K. The circles at lower temperature correspond to cusps in M which seem to be related to a reduction in the WFM behavior; circles at 20 K represent cusps associated with complete disappearance of the WFM behavior.

$Gd_{1.85}Ce_{0.15}CuO_{4-y}$ has previously been shown[35,57] to exhibit Cu AFM order at 150 K. As seen in Fig. 7, the anomaly due to Cu AFM order is somewhat depressed in temperature as Nd is substituted for Gd, although a concomitant broadening of the anomaly makes it difficult to extract T_N. Similar to the Ce-undoped system, lower temperature cusps associated with a reduction and disappearance, respectively, of the WFM behavior are observed. Here we see another example of separation between Cu AFM order and

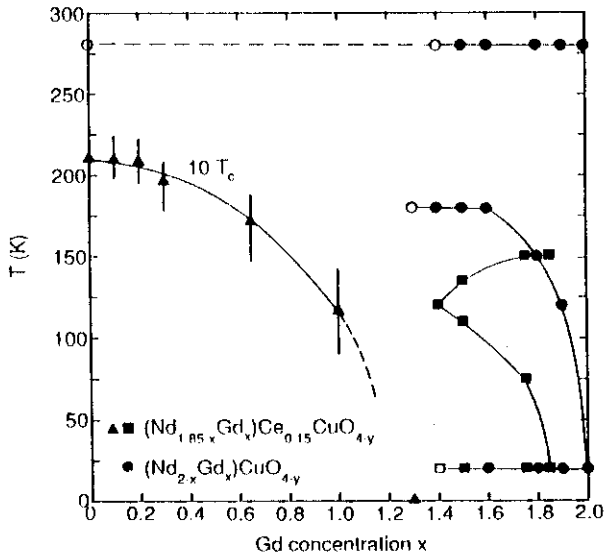

Fig. 7. Temperature-Gd concentration (T-x) phase diagram of $(Nd_{2-x}Gd_x)CuO_{4-y}$ and $(Nd_{1.85-x}Gd_x)Ce_{0.15}CuO_{4-y}$. Triangles represent the 50% resistive T_c's for the Ce-doped compounds. Vertical bars on these points represent the 10% - 90% transition widths. Filled squares (Ce-doped) and circles (no Ce) represent temperatures at which anomalies are observed in the low-H magnetization M as described in the text. Solid lines are guides to the eye. Not shown are Néel temperatures for AFM ordering of the Nd and Gd ions which are less than 7 K.

superconductivity, although the precise behavior of the magnetic phase boundary is difficult to determine in this system by this method.

Pressure dependence of T_c : Electron/hole antisymmetry

The pressure dependence of T_c of the electron-doped superconductors differs significantly from that of their hole-doped counterparts. In the hole-doped superconductors, an increase of T_c with nearly hydrostatic pressure below ~20 kbar has generally been reported.[60-65] However, for the electron-doped system, both an absence of a pressure effect[65] or, at most, a small positive pressure effect[29] on T_c have been reported for $Nd_{1.85}Ce_{0.15}CuO_{4-y}$, while a small, negative pressure effect[35] has been observed for $Nd_{1.85}Th_{0.15}CuO_{4-y}$.

An extensive study[66] of the pressure dependence of T_c for all seven known cation-substituted electron-doped superconductors $Ln_{2-x}M_xCuO_{4-y}$ reveals that except, perhaps, for the highest-T_c specimen, dT_c/dP is negative. This is in sharp contrast to the positive values of dT_c/dP observed for the hole-doped copper-oxide superconductors. In Fig. 8, the relative rate of change of T_c (defined as the temperature at which ρ drops to 90% of its maximum value just above T_c) with pressure, $d\ln T_c/dP$, is plotted versus T_c. The right scale of the figure expresses the results in terms of $d\ln T_c/d\ln V$, which is more

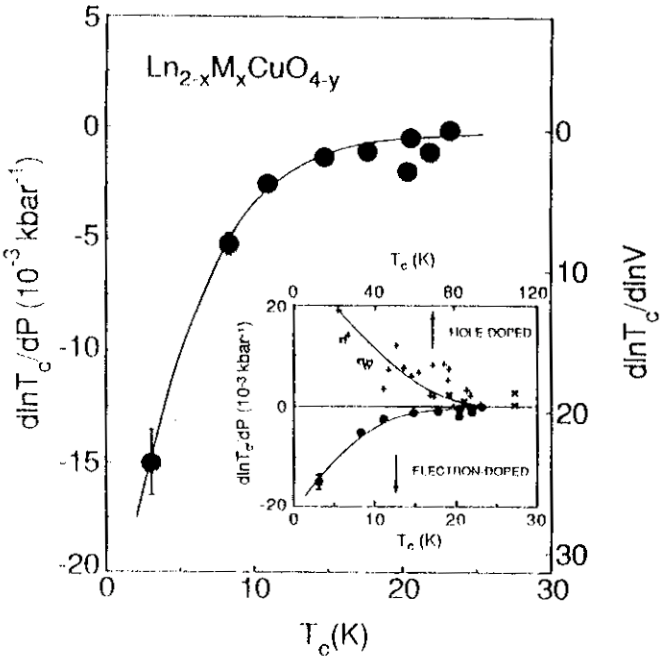

Fig. 8. Relative rate of change of T_c (90% point) with applied pressure P, $dlnT_c/dP$, as a function of T_c for the electron-doped superconductors. Inset: Same data plotted together with similar data for hole-doped superconductors from Ref. 65. (□ : La-based "214", + : R-based "123", and x : Bi-Sr- and Tl-Ba Ca-Cu-O materials.) From Ref. 66.

accessible to theoretical models,[60] under the assumption that the bulk modulus has a value B ≈ 1600 kbar, as for La_2CuO_4.[67] Several important points warrant attention. Most notably, the $dlnT_c/dP$ data are predominantly negative, in contrast to the general trend for the hole-doped copper-oxide superconductors, shown in the inset of Fig. 8, although the shapes of the curves are similar for both systems. For a successful theory of superconductivity in the copper oxides to encompass both systems, this antisymmetric pressure dependence of T_c must be accomodated.

The magnitude of $dlnT_c/dP$ is small for samples with T_c near the maximum value obtained for the electron-doped materials ($T_c \approx 24$ K); however, for low T_c values, $|dlnT_c/dP|$ can be quite large, similar to the maximum magnitude observed in the hole-doped compounds. These large values cannot be explained in the framework of the BCS theory with electron-phonon interaction.[60] Finally, the fact that $dlnT_c/dP$ becomes very small near the highest T_c so far obtained in both electron- and hole-doped materials may indicate that electron-doped compounds have a maximum $T_c \approx 25$ K.

Anisotropic upper critical field of $Sm_{1.85}Ce_{0.15}CuO_{4-y}$: Interaction between superconductivity and antiferromagnetic order

Recently, the temperature dependence of the anisotropic upper critical field $H_{c2}(T)$ was determined resistively for single crystal specimens of $Ln_{2-x}Ce_xCuO_{4-y}$ for Ln = Nd, x = 0.14 (Ref. 68) and Ln = Sm, x = 0.15 (Ref. 69). The H_{c2} vs T data for the $Sm_{1.85}Ce_{0.15}CuO_{4-y}$ single crystal reveal an enhancement of $H_{c2}(T)$ below the Néel temperature T_N where the Sm^{3+} ions undergo an AFM transition, providing the first evidence in high T_c copper oxides for the interaction between superconductivity and AFM ordering of Ln ions. This observation could be helpful in identifying the superconducting electron pairing mechanism in the family of electron-doped superconductors.

The temperature dependence of the electrical resistivity ρ in the basal plane for a $Sm_{1.85}Ce_{0.15}CuO_{4-y}$ single crystal exhibits metallic behavior which is similar to that recently reported for a $Nd_{1.84}Ce_{0.16}CuO_{4-y}$ single crystal,[68] reminiscent of ordinary metals and qualitatively different from that of hole-doped superconductors. The superconducting transition temperature T_c, defined as the temperature at which ρ drops to 50% of its extrapolated normal state value, is 11.4 K, while the 10%–90% transition width is 2.7 K.

With increasing applied magnetic field, there is a striking parallel shift of the transition curves to lower temperatures for both H directions; the transition widths remain essentially constant as in conventional type II superconductors. In contrast to other high-T_c cuprates where the determination of H_{c2} is complicated by substantial field-induced broadening of the resistive transitions, presumably due to dissipative flux motion[70] or to fluctuation effects,[71] in this case H_{c2} is well defined.

The $H_{c2}(T)$ curves obtained from the ρ(T,H) data reveal a large anisotropy with H_{c2} largest for $H \perp c$, typical of layered compounds. For $H \perp c$, the $H_{c2}(T)$ curve exhibits a slight upward curvature near T_c; the initial slope $(-dH_{c2}/dT)$, estimated by ignoring this curvature, is 3.6 T/K. For $H \| c$, $H_{c2}(T)$ exhibits positive curvature throughout the whole temperature range with initial slope $(-dH_{c2}/dT) = 0.1$ T/K, as estimated from the data below 11 K. For $H \perp c$, the steep slope of $H_{c2}(T)$ and the higher temperatures imply that paramagnetic effects are small, and the weak coupling formula[72] can be used to estimate $H_{c2}(0) = -0.69\ T_c\ (dH_{c2}/dT)_{T=Tc} \approx 28.2$ T. For $H \| c$, the extrapolated value $H_{c2}(0) = 5.23$ T, can be used as justified below. The Ginzburg-Landau coherence lengths deduced from these $H_{c2}(0)$ values are $\xi_{ab} = 80$ Å and $\xi_c = 15$ Å. The anisotropy factor is about 5 and results in an effective mass ratio $m_c/m_{ab} \approx 29$. This intrinsic anisotropy is smaller than found in Ref. 68; the large factor (~21) determined in that study is most likely an artifact of the magnetic pair breaking contribution of the Nd^{3+} ions, similar to that of the Sm^{3+} ions discussed below. Of particular importance is the large value of the coherence length within the CuO_2 planes which increases the pinning energy according to the scaling theory of Anderson and Kim[73] and could account for the parallel shift behavior of the resistive transitions. Corresponding values of ξ_{ab} in hole-doped copper oxide superconductors range between 13 and 40 Å. Positive curvatures in $H_{c2}(T)$ curves have been widely reported in high-T_c cuprates and generally accounted for by flux creep dissipation or fluctuation effects; however, these effects are usually accompanied by resistive broadening not observed here.

In Fig. 9(a), normalized $H_{c2}(T)$ data for $Sm_{1.85}Ce_{0.15}CuO_{4-y}$ (Ref. 69) and $Nd_{1.84}Ce_{0.16}CuO_{4-y}$ (Ref. 68) single crystals are plotted versus reduced temperature T/T_c, for $H \| c$. Two extraordinary features are found in this plot. First, the normalized $H_{c2}(T)$ data for both systems scale with T/T_c for $T/T_c \geq 0.5$ and consequently, can be described by a single equation, $H_{c2}(T) = H^{\prime}_{c2}(0)\ (1 - T/T_c)^{1.6}$. Second, there is a sudden departure of the $Sm_{1.85}Ce_{0.15}CuO_{4-y}$ $H_{c2}(T)$ data from the behavior predicted by this scaling and

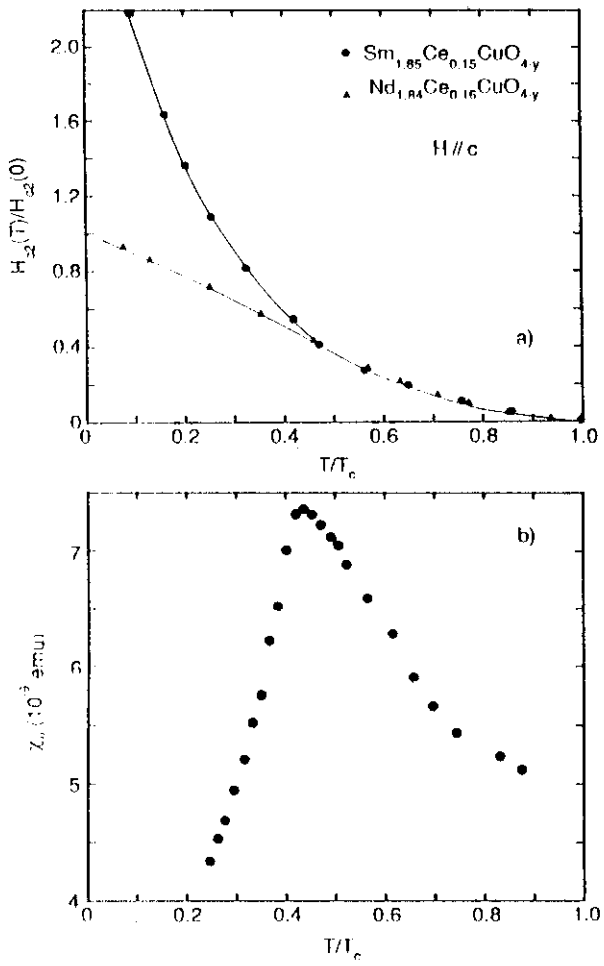

Fig. 9. (a) Normalized upper critical magnetic field $H_{c2}(T)/H^{\dagger}_{c2}(0)$ vs reduced temperature T/T_c for $Sm_{1.85}Ce_{0.15}CuO_{4-y}$ and $Nd_{1.84}Ce_{0.16}CuO_{4-y}$ (Ref. 68) single crystals for H||c where $H^{\dagger}_{c2}(0)$ equals 1.83 T and 7.0 T, respectively. (b) Magnetic susceptibility χ vs T/T_c for $Sm_{1.85}Ce_{0.15}CuO_{4-y}$ single crystals measured in an applied magnetic field of 1 T parallel to the c-axis. From Ref. 69.

followed by the $Nd_{1.84}Ce_{0.16}CuO_{4-y}$ $H_{c2}(T)$ data for $T/T_c \lesssim 0.5$. This increase in $H_{c2}(T)$ correlates with a sharp drop near $T_N = 4.9$ K in the static magnetic susceptiblity for H|| c, shown in Fig. 9(b). Unequivocal evidence for bulk long-range antiferromagnetic ordering of the Sm^{3+} ions along the c-axis near T_N has already been found in specific heat and magnetic susceptibility measurements on both single crystal and polycrystalline specimens of Sm_2CuO_4 and superconducting $Sm_{1.85}Ce_{0.15}CuO_{4-y}$.[74,75] This, along with the fact

that T_N in the $Sm_{1.85}Ce_{0.15}CuO_{4-y}$ single crystal does not vary significantly with applied magnetic fields to 4 T, demonstrates that the peak in the magnetic susceptibility shown in Fig. 9(b) is associated with the antiferromagnetic ordering of Sm^{3+} ions along the c-axis. The effect of magnetic ordering on the upper critical field in $Sm_{1.85}Ce_{0.15}CuO_{4-y}$ clearly indicates that there is a significant interaction between the rare earth magnetic moments and the superconducting charge carriers.

In the context of the multiple pair-breaking theory, the anomalous increase in $H_{c2}(T)$ for $H \| c$ in $Sm_{1.85}Ce_{0.15}CuO_{4-y}$ can be explained in terms of a reduction of the magnetization and, in turn, of the exchange field associated with the Sm spins and a corresponding decrease in its pair breaking effect on the conduction electron spins through the Zeeman interaction. In order to deduce the exchange coupling, the orbital critical field $H_{c2}^*(T)$ has been approximated by $H_{c2}^*(T) \approx H_{c2}^*(0)\,(1 - T/T_c)^{\beta}$ and required to satisfy $H_{c2}^*(0) \approx H_{c2}(0)$, since the Sm^{3+} magnetization at $T = 0$ will be zero for $H \| c$. Estimating the exchange field $H_J(T)$ due to the Sm^{3+} ions at the Néel temperature T_N where it is maximum[76] yields $H_J(T_N) \approx 90$ kOe (160 kOe), corresponding to an exchange coupling constant $J \approx 60$ meV (110 meV), for $\beta = 2$ (1). This is about a factor of four greater than that observed in $SmRh_4B_4$, and reflects a stronger rare-earth-conduction-electron coupling in the layered copper-oxide compound.

Acknowledgements

The support of the U. S. Department of Energy under Grant No. DE-FG03-86ER45230 and the U. S. National Science Foundation under Grant No. DMR-8411839 and Grant No. DMR-8803185 are gratefully acknowledged.

References

1. J. G. Bednorz and K. A. Müller, *Z. Phys. B* **64** (1986) 189.
2. For a review, see J. T. Markert, Y. Dalichaouch, and M. B. Maple, in *Physical Properties of High Temperature Superconductors I*, ed. D. M. Ginsberg (World Scientific, Singapore, 1989), p. 266.
3. M. B. Maple, J. M. Ferreira, R. R. Hake, B. W. Lee, J. J. Neumeier, C. L. Seaman, K. N. Yang, and H. Zhou, *J. Less-Common Metals* **149** (1989) 405.
4. L. Soderholm, K. Zhang, D. G. Hinks, M. A. Beno, J. D. Jorgensen, C. U. Segre, and I. K. Schuller, *Nature* **328** (1987) 604.
5. J. K. Liang, X. T. Xu, S. S. Xie, G. H. Rao, X. Y. Shao, and Z. G. Dian, *Z. Phys. B* **69** (1987) 137.
6. Y. Dalichaouch, M. S. Torikachvili, E. A. Early, B. W. Lee, C. L. Seaman, K. N. Yang, H. Zhou, and M. B. Maple, *Solid State Commun.* **65** (1988) 1001; and references therein.
7. J. J. Neumeier, M. B. Maple, and M. S. Torikachvili, *Bull. Am. Phys. Soc.* **33** (1988) 689; *Physica C* **156** (1988) 574.
8. A. Kebede, C.-S. Jee, J. Schwegler, J. E. Crow, T. Mihalisin, G. H. Myer, R. E. Salomon, P. Schlottmann, M. V. Kuric, S. H. Bloom, and R. P. Guertin, *Phys. Rev. B* **40** (1989) 4453; and references therein.
9. J. L. Peng, P. Klavins, R. N. Shelton, H. B. Radousky, P. A. Hahn, and L. Bernardez, *Phys. Rev. B* **40** (1989) 4517.
10. J. J. Neumeier, T. Bjørnholm, M. B. Maple, and I. K. Schuller, *Phys. Rev. Lett.* **63** (1989) 2516.

11. J. J. Neumeier, *Ph. D. Thesis*, University of California, San Diego, 1989 (unpublished).
12. S. Ghamaty, B. W. Lee, J. J. Neumeier, G. Nieva, and M. B. Maple, to be published.
13. J.-S. Kang, J. W. Allen, Z.-X. Shen, W. P. Ellis, J. J. Yeh, B. W. Lee, M. B. Maple, W. J. Spicer, and I. Lindau, *J. Less Comm. Met.* **24** (1989) 25.
14. J. J. Neumeier, T. Bjørnholm, M. B. Maple, J. J. Rhyne, and J. A. Gotaas, *Physica C* **166** (1990) 191.
15. A. Matsuda, K. Kineshita, T. Ishii, H. Shibata, T. Watanabe, and T. Yamada, *Phys. Rev. B* **38** (1988) 2910.
16. A. P. Goncalves, I. C. Santos, E. B. Lopes, R. T. Henriques, H. Almeida, and M. O. Figueiredo, *Phys. Rev. B* **37** (1988) 7476.
17. E. E. Alp, G. K. Shenoy, L. Soderholm, G. L. Goodman, D. G. Hinks, and B. W. Veal, *Mat. Res. Soc. Symp.* **99** (1988) 177.
18. D. W. Cooke, R. S. Kwok, R. L. Lichti, T. R. Adams, C. Boekema, W. K. Dawson, A. Kebede, J. Schwegler, J. E. Crow, and T. Mihalisin, *Phys. Rev. B* **41** (1990) 4801.
19. I. Felner, U. Yaron, I. Nowik, E. R. Bauminger, Y. Wolfus, E. R. Yacoby, G. Hischer, and N. Pillmayr, *Phys. Rev. B* **40** (1989) 6739.
20. M. B. Maple, *Appl. Phys.* **9** (1976) 179.
21. M. B. Maple, L. M. Paulius, and J. J. Neumeier, to be published.
22. J. Fink, N. Nücker, H. Romberg, M. Alexander, M. B. Maple, J. J. Neumeier, and J. W. Allen, to be published.
23. J. Souletie, *J. de Physique* **49** (1988) 1211.
24. A. W. Sleight, *Science* **242** (1988) 1519.
25. Y. Tokura, H. Takagi, and S. Uchida, *Nature* **337** (1989) 345.
26. J. T. Markert and M. B. Maple, *Solid State Commun.* **70** (1989) 145.
27. A. C. W. P. James, S. M. Zahurak, and D. W. Murphy, *Nature* **338** (1989) 240.
28. A. Khurana, *Physics Today* **42** (1989) 17.
29. J. T. Markert, E. A. Early, T. Bjørnholm, S. Ghamaty, B. W. Lee, J. J. Neumeier, R. D. Price, C. L. Seaman, and M. B. Maple, *Physica C* **158** (1989) 178.
30. E. A. Early, N. Y. Ayoub, J. Beille, J. T. Markert, and M. B. Maple, *Physica C* **160** (1989) 320.
31. I. Felner, U. Yaron, Y. Yeshurun, E. R. Yacoby, and Y. Wolfus, *Phys. Rev. B* **40** (1989) 11366.
32. N. Y. Ayoub, E. A. Early, J. T. Markert, C. L. Seaman, and M. B. Maple, to be published.
33. Y. J. Uemura, G. M. Luke, B. J. Sternlieb, L. P. Le, J. H. Brewer, R. Kadono, R. F. Kiefl, S. R. Kreitzman, T. M. Riseman, C. L. Seaman, J. J. Neumeier, Y. Dalichaouch, M. B. Maple, G. Saito, and H. Yamochi, to be published in the Proceedings of the NATO Advanced Research Workshop on *Dynamics of Magnetic Fluctuations in High Temperature Superconductors*, Crete, October, 1990 (Plenum, 1990).
34. G. M. Luke, B. J. Sternlieb, Y. J. Uemura, J. H. Brewer, R. Kadono, R. F. Kiefl, S. R. Kreitzman, T. M. Riseman, J. Gopalakrishnan, A. W. Sleight, M. A. Subramanian, S. Uchida, H. Takagi, and Y. Tokura, *Nature* **338** (1989) 49.
35. C. L. Seaman, N. Y. Ayoub, T. Bjørnholm, E. A. Early, S. Ghamaty, B. W. Lee, J. T. Markert, J. J. Neumeier, P. K.Tsai, and M. B. Maple, *Physica C* **159** (1989) 391.
36. A. Butera, A. Caneiro, M. T. Causa, L. B. Steren, R. Zysler, M. Tovar, and S. B. Oseroff, *Physica C* **160** (1989) 341.

37. J. B. Torrance, Y. Tokura, A. I. Nazzal, A. Bezinge, T. C. Huang, and S. S. P. Parkin, *Phys. Rev. Lett.* **61** (1988) 1127.
38. N. Y. Ayoub, J. T. Markert, E. A. Early, C. L. Seaman, L. M. Paulius, and M. B. Maple, *Physica C* **165** (1990) 469.
39. H. Takagi, S. Uchida, and Y. Tokura, *Phys. Rev. Lett.* **62** (1989) 1197.
40. S. Uchida, H. Takagi, and Y. Tokura, *Physica C* **162-164** (1989) 1677.
41. Z. Z. Wang, T. R. Chien, N. P. Ong, J. M. Tarascon, and E. Wang, to be published.
42. A. Weidinger, C. Niedermayer, A. Golnik, R. Simon, E. Recknegal, J. I. Budnick, B. Chamberland, and C. Baines, *Phys. Rev. Lett.* **62** (1989) 102.
43. T. Oguchi and T. Obokata, *J. Phys. Soc. Jpn.* **27** (1969) 1111.
44. G. Liang, J. Chen, M. Croft, K. V. Ramanujacharay, M. Greenblatt, and M. Hegde, *Phys. Rev. B* **40** (1989) 2646.
45. S. Uji, M. Shimoda, and H. Aoki, *Jpn. J. Appl. Phys.* **28** (1989) L804.
46. J. M. Tranquada, S. M. Heald, A. R. Moodenbaugh, G. Liang, and M. Croft, *Nature* **337** (1989) 720.
47. A. Fujimori, Y. Tokura, H. Eisaki, H. Takagi, S. Uchida, E. Takayama-Muromachi, *Phys. Rev. B*, submitted.
48. E. E. Alp, S. M. Mini, M. Ramanathan, B. Dabrowski, D. R. Richards, and D. G. Hinks, *Phys. Rev. B* **40** (1989) 2617.
49. M. K. Rajumon, D. D. Sarma, R. Vijayaraghavan, and C. N. R. Rao, *Solid State Commun.* **70** (1989) 875.
50. N. Nücker, P. Adelmann, M. Alexander, H. Romberg, S. Nakai, J. Fink, H. Rietschel, G. Roth, H. Schmidt, and H. Spille, *Z. Phys. B* **75** (1989) 421.
51. S. Massida, N. Hamada, J. Yu, and A. J. Freeman, *Physica C* **157** (1989) 571.
52. J. W. Allen, C. G. Olsen, M. B. Maple, J.-S. Kang, L. Z. Liu, J.-H. Park, R. O. Anderson, W. P. Ellis, J. T. Markert, Y. Dalichaouch, and R. Liu, *Phys. Rev. Lett.* **64** (1990) 595.
53. T. C. Huang, E. Moran, A. I. Nazzal, J. B. Torrance, and P. W. Wang, *Physica C* **159** (1989) 625.
54. P. H. Hor, Y. Y. Xue, Y. Y. Sun, Y. C. Tao, Z. J. Huang, W. Rabalais, and C. W. Chu, *Physica C* **159** (1989) 629.
55. A. Grassman, J. Schlötterer, J. Ströbel, M. Klauda, R. L. Johnson, and G. Saemann-Ischenko, *Physica C* **162-164** (1989) 1383.
56. J. D. Thompson, S-W. Cheong, S. E. Brown, Z. Fisk, S. B. Oseroff, M. Tovar, D. C. Vier, and S. Schultz, *Phys. Rev. B* **39** (1989) 6660.
57. I. Dzyaloshinski, *J. Phys. Chem. Solids* **4** (1958) 241.
58. T. Moriya, *Phys. Rev.* **120** (1960) 91.
59. S. B. Oseroff, D. Rao, F. Wright, D. C. Vier, S. Schultz, J. D. Thompson, Z. Fisk, S-W. Cheong, M. F. Hundley, and M. Tovar, *Phys. Rev. B* **41** (1990) 1934.
60. R. Griessen, *Phys. Rev. B* **36** (1987) 5284.
61. N. Tanahashi, Y. Iye, T. Tamegai, C. Murayama, N. Môri, S. Yomo, N. Okazaki, and K. Kitazawa, *Jpn. J. Appl. Phys.* **28** (1989) L762.
62. M. C. Aronson, S-W. Cheong, F. H. Garzon, J. D. Thompson, and Z. Fisk, *Phys. Rev. B* **39** (1989) 11445.
63. M. B. Maple, Y. Dalichaouch, E. A. Early, B. W. Lee, J. T. Markert, J. J. Neumeier, C. L. Seaman, K. N. Yang, and H. Zhou, *Physica C* **153–155** (1988) 858.
64. J. E. Shirber, B. Morosin, and D. S. Ginley, *Physica C* **157** (1989) 237.
65. C. Murayama, N. Môri, S. Yomo, H. Takagi, S. Uchida, and Y. Tokura, *Nature* **339** (1989) 293.
66. J. T. Markert, J. Beille, J. J. Neumeier, E. A. Early, C. L. Seaman, T. Moran, and M. B. Maple, *Phys. Rev. Lett.* **64** (1990) 80.

67. H. Takahashi, C. Murayama, S. Yomo, N. Môri, K. Kishio, K. Kitazawa, and K. Fueki, *Jpn. J. Appl. Phys.* **26** (1987) L504.
68. Y. Hidaka and M. Suzuki, *Nature* **338** (1989) 635.
69. Y. Dalichaouch, B. W. Lee, C. L. Seaman, J. T. Markert, and M. B. Maple, *Phys. Rev. Lett.* **64** (1990) 599.
70. Y. Yeshurun and A. P. Malozemoff, *Phys. Rev. Lett.* **60** (1988) 2202.
71. S. Kambe, M. Naito, K. Kitazawa, I. Tanaka, and H. Kojima, *Physica C*, submitted.
72. R. R. Hake, *Appl. Phys. Lett.* **10** (1967) 186.
73. P. W. Anderson, *Phys. Rev. Lett.* **9** (1962) 309; Y. B. Kim, *Rev. Mod. Phys.* **36** (1964) 39.
74. M. B. Maple, N. Y. Ayoub, T. Bjørnholm, E. A. Early, S. Ghamaty, B. W. Lee, J. T. Markert, J. J. Neumeier, and C. L. Seaman, *Physica C* **162-164** (1989) 296.
75. M. F. Hundley, J. D. Thompson, S-W. Cheong, and Z. Fisk, *Physica C* **158** (1989) 102.
76. Ø. Fischer, M. Ishikawa, M. Pelizzone, and A. Treyvaud, *J. de Phys. Colloq.* **40** (1979) C5-89.